Inorganic Chemistry Communications 183 (2026) 115818

Contents lists available at ScienceDirect

Inorganic Chemistry Communications

journal homepage: www.elsevier.com/locate/inoche

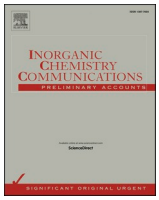

Research Article

A strategic framework for zinc oxide electrochemical synthesis using design of experiments

Margherita Izzi [a,b], Alessandro Faranda [a], Rosaria Anna Picca [a,b], Gennaro Ventruti [c], Barbara Giussani [d,*], Nicola Cioffi [a,*]

[a] Dipartimento di Chimica, Università degli Studi di Bari Aldo Moro, Via E. Orabona 4, 70126 Bari, Italy
[b] CNR-Istituto di Fotonica e Nanotecnologie, Italy
[c] Dipartimento Di Scienze Della Terra E Geoambientali, Via E. Orabona 4, 70126 Bari, Italy
[d] Dipartimento di Scienza e Alta Tecnologia, Università degli Studi dell'Insubria, Via Valleggio 11, 22100 Como, Italy

ARTICLE INFO

Keywords:
ZnO
Electrosynthesis
Response surface methodology
Optimization
Scale-up

ABSTRACT

Electrochemical methods have gained increasing attention for the synthesis of micro- and nanostructured materials such as zinc oxide (ZnO). Traditionally, the development of such syntheses has relied on the One Variable At a Time (OVAT) approach, which systematically changes a single parameter while keeping others constant. However, this method provides only a limited understanding of the multidimensional experimental space. In contrast, a Design of Experiments (DoE) strategy offers a more efficient and statistically robust framework for identifying optimal synthesis conditions. In this work, we propose the application of a Full Factorial Design combined with Response Surface Methodology (RSM) to optimize for the first time the electrochemical synthesis of ZnO structures. The synthetic strategy integrates a hybrid electrochemical–thermal process: sacrificial zinc electrolysis in a 30 mM sodium hydrogen carbonate solution, followed by thermal annealing that is typically employed in sol–gel methods to gain a final control over stoichiometry and morphology. ZnO microrods (ZnO MRs) were synthesized under galvanostatic conditions using benzalkonium chloride as a cationic surfactant and stabilizer. Its concentration (0.001–0.5 M) and the applied current density (2–20 mA/cm^2) were selected as the key variables. A two-factor, three-level Central Composite Design (CCD) was implemented to investigate their combined effects on the electrosynthesis yield and ZnO length. The predictive model derived from the chemometric analysis was successfully validated, demonstrating the method's potential for rational and efficient optimization of nano- and micromaterial electrosynthesis. Moreover, the proposed model was also validated on a scaled-up system, proving effective not only for laboratory-scale optimization but also for guiding process development toward industrial applications, where control, reproducibility, and efficiency are critical.

1. Introduction

The exceptional properties and remarkable versatility of ZnO are well established and widely recognized within the materials science community. Depending on the synthesis approach and experimental conditions, micro- and nanostructured ZnO particles can be tailored into various morphologies. This tunability enables a broad spectrum of applications, including catalysis [1], environmental remediation [2], drug delivery [3], and personal care products [4]. The most popular approaches are based on sol-gel technologies [5,6], whereas more recently, electrochemical routes have attracted increasing interest as a sustainable and controllable alternative for material development. Since 2015, we have worked on electrochemical sol-gel strategies, based on a sacrificial zinc electrolysis in a sodium hydrogen carbonate solution (30 mM) [7]. By varying different stabilizers, we successfully tuned the ZnO morphology, obtaining spheroidal nanoparticles [7], nano- and microrods [8], and microflowers [9], thus demonstrating the versatility of this approach. However, the investigation of these synthetic procedures to determine the best experimental parameters was carried out by changing one parameter at a time, while keeping all other variables constant, following the so-called One Variable At a Time (OVAT) method. Although widely used, this approach does not enable true optimization, as it explores only a one-dimensional parameter space, potentially failing to identify the actual optimum [10]. In contrast, the combination

* Corresponding authors.
E-mail addresses: barbara.giussani@uninsubria.it (B. Giussani), nicola.cioffi@uniba.it (N. Cioffi).

https://doi.org/10.1016/j.inoche.2025.115818
Received 3 September 2025; Received in revised form 28 October 2025; Accepted 6 November 2025
Available online 7 November 2025

of Design of Experiments (DoE) and Response Surface Methodology (RSM) offers an efficient and comprehensive framework for the multivariate investigation and optimization of materials synthesis. This approach not only promotes a clearer understanding of the synthetic system but also highlights the key experimental variables. DoE is a multivariate strategy designed to maximize the ratio between the quality of information gained about a chemical system or process and the experimental effort required. This is achieved through the rational planning and selection of experiments to extract the most meaningful knowledge from a limited number of experiments [11,12]. RSM, on the other hand, encompasses a set of mathematical and statistical techniques that fit a polynomial equation to experimental data, aiming to describe system behavior and enable statistical prediction [13]. It is particularly effective when one or more responses of interest are influenced by multiple variables - an almost universal scenario for materials chemists and experimental scientists in general. By facilitating systematic analysis and multidimensional modeling of factor effects on targeted responses, RSM allows for the optimization of complex synthetic spaces with significantly fewer experimental runs. Despite the growing adoption of data-driven chemometric tools in the current materials science community, their application to electrochemical synthesis methods remains surprisingly limited and underexplored. So and colleagues [14] and Anand & Srivastava [15] similarly applied the Taguchi design to optimize parameters such as pH, concentration, voltage, and conductivity during the electrosynthesis of ZnO nanorods, aiming to enhance yield while minimizing energy and electrode consumption. However, their method employed oxalic acid as a reducing agent, which may pose potential safety issues, and required relatively high potentials (2–8 V). The Taguchi method have also been used in the optimization of other electrochemical or electrodeposition systems, for instance to optimize the diameter of silver tungstate nanoparticles [16], the size of copper tungstate particles [17] and nickel sulfide particles [18]. While effective for screening large numbers of factors with minimal experimental effort [19], the Taguchi approach does not identify interactions between variables which significantly limits its capacity to unravel the multivariate relationships that govern complex electrochemical syntheses. Among the experimental matrices available for optimizing experiments, central composite design (CCD) is a classic design matrix for fitting second-order models. The main advantage of CCD is that it allows for efficient estimation of main effects and interactions, providing useful information about the linear and interaction effects of the factors [20,21]. The design points are strategically placed on the faces of the factorial cube and in the center, allowing for a balanced and efficient exploration of the factor space. Despite its proven strength in modeling nonlinear and interactive effects, CCD has been rarely applied to electrochemical synthesis processes, and, to our knowledge, never to the electrosynthesis of ZnO structures. For instance, Gerard and colleagues reported the use of a central composite design to optimize the electrodeposition of cobalt–copper phosphate electrodes [22]. Building on this gap, the present work introduces for the first time the use of a central composite design for the rational optimization of the electrosynthesis of ZnO microrods (ZnO MRs). By coupling a statistically rigorous CCD framework with electrochemical synthesis, we demonstrate a data-driven strategy capable of capturing complex variable interactions and providing a more predictive understanding of process–structure relationships. This approach establishes a methodological advancement over traditional Taguchi-based optimizations, marking a novel step toward the integration of chemometric intelligence in electrochemical materials design. Using the aforementioned eco-friendly sodium bicarbonate-based electrolyte, ZnO MRs were synthesized under galvanostatic conditions, with moderate current densities (up to 20 mA/cm^2). Although the influence of experimental parameters on such synthetic process products has already been OVAT investigated over the past decade, this study offers new insights by applying chemometric tools to rationalize and quantify the effects of two critical variables: the concentration of the stabilizer, and the applied current density. Benzalkonium chloride, a cationic surfactant known to induce anisotropic growth along the c-axis and promote rod-like ZnO morphologies [8], was chosen as the stabilizer. Its concentration was varied from 0.001 M to 0.5 M, whereas the applied current density ranged from 2 to 20 mA/cm^2. A two-factor three-level Central Composite Design was implemented to explore and model the system's behavior. Specifically, the face-centered CCD was employed to optimize the electrosynthesis yield of ZnO microstructures and to rationalize their size. The model was successfully validated, both for lab-scale and scaled-up systems. This approach offers a more environmentally conscious and resource-efficient strategy compared to traditional techniques, characterized by a reduced experimental workload and effort, for identifying the optimal conditions that maximize ZnO yield and control particle size, providing a transferable and innovative framework for optimizing material synthesis via sustainable electrochemical routes.

2. Materials and methods

2.1. Materials

Zinc and platinum sheets (1 mm thick, 99.99 + %) were purchased from Goodfellow LTD and cut into 2 × 1 cm^2 pieces. Sodium hydrogen carbonate ($NaHCO_3$, purum p.a., 99.0 %), hydrochloric acid (HCl, ACS reagent, 37 %), benzyl-hexadecyl-dimetylammonium chloride (BAC, pure cationic surfactant), were purchased from Merck Sigma–Aldrich (Milan, Italy). Polishing suspensions with different nominal abrasive sizes were purchased from Buehler.

2.2. Synthesis and characterization of ZnO MRs

ZnO MRs were synthesized using a green and scalable electrochemical procedure developed in our laboratories [8]. Aqueous electrosynthesis was conducted under mild galvanostatic conditions in the presence of benzyl-hexadecyl-dimetylammonium chloride (BAC). A three-electrode cell was utilized, lying on a Zn sheet as the working electrode, a Pt sheet as the counter electrode, and Ag/AgCl (KCl sat.) as the reference electrode. Zn plate (2,5 × 1 cm^2) was initially polished using sandpaper and then using polishing slurries at decreasing granulometry. After sonication in MilliQ water, it was immersed in 1 M HCl for 30 s to ensure activation. Different current density values were applied, using a CH − 1140b potentiostat–galvanostat (CH Instruments, Bee Cave, TX, USA). The synthesis was carried out at room temperature, using 7 mL of 30 mM $NaHCO_3$ aqueous solution as electrolytic medium with different concentration of BAC according to the experimental design (vide infra), under stirring conditions (700 rpm). A Teflon spacer (4 mm thick) was used to maintain a constant interelectrode distance throughout the experiments. To ensure a constant amount of zinc release, the synthesis time was calculated as a function of the applied current density, according to Faraday's law. After the synthesis, the colloidal dispersion was centrifuged at 6000 rpm for 20 min.

For the scale-up system, two zinc sheets 5 × 5 cm^2 were used as working and counter electrodes, keeping an Ag/AgCl (KCl sat.) as reference electrode. The electrochemical synthesis was carried out at room temperature using 400 mL of hydrogen carbonate-based electrolytic bath.

The precipitates were dried overnight at 120 °C. The dried validation samples were also calcined, a typical step in sol–gel processes used to convert zinc compounds into pure zinc oxide. Both the lab-scale and the scaled-up samples were calcined at 450 °C; however, the former was treated for 1 h, while the latter required 4 h due to the larger sample amount.

Bulk chemical composition of the powders was obtained by attenuated total reflectance infrared (ATR-FTIR) analysis on a Spectrum Two FTIR spectrometer (PerkinElmer, Milan, Italy) with a resolution of 2 cm^{-1} scanning from 4000 to 400 cm^{-1}. A total of 16 scans were averaged; background spectra were acquired against air, and spectral

Table 1
Independent variables and level used in DoE experimentation.

Independent variables (X_i)	-1	0	+1
BAC concentration	0.001 M	0.25 M	0.5 M
Current density (j)	2 mA/cm^2	10 mA/cm^2	20 mA/cm^2

Table 2
Experimental conditions at the validation points for lab-scale and scale-up syntheses of ZnO MRs.

Experimental conditions for the validation points	Laboratory scale	Scale up
electrolyte volume (mL)	7	400
electrode area (cm^2)	2.5	12.5
current density (mA/cm^2)	15.5	10
synthesis time (min)	40	180
BAC concentration	0.1	0.01
stirring	700 rpm	700 rpm

baseline subtraction was performed using instrument software. UV–Vis spectra were acquired by a Shimadzu UV-1601 double beam spectrometer with 1 cm quartz Suprasil® cuvettes. The ZnO MR morphology was studied by transmission electron microscopy (TEM, FEI Tecnai 12, Hillsboro, OR, USA; high tension: 120 kV; filament: LaB_6). Particle size analysis was performed with ImageJ software (http://imagej.nih.gov/ij/). X-ray powder diffraction (XRPD) data were collected using an Empyrean PANalytical diffractometer equipped with a 1.8 kW CuKα ceramic X-ray tube (λ_{avg} = 1.5418 Å) and a real-time multiple strip (RTMS) PIXcel3D detector. The sample was loaded onto a zero-background holder (ZBH) made from single-crystal silicon, cut at a specific orientation parallel to the Si (510) plane. Analytical conditions were: 40 mA and 40 kV, a scanning speed of 0.026°/s, and a 2θ range from 15° to 80°. The system included a set of narrow slits: a 0.0625° divergence slit, a 0.125° antiscatter slit, and 0.02 rad Soller slits. Multiple scans were combined to improve the signal-to-noise ratio.

Table 3
Runs and response variables of a face-centered CCD model with three levels of BAC concentration and current density j.

Run	Independent variables (X_i)		Responses (Y_i)	
	BAC (M)	*j (mA/cm^2)*	*Yield (%)*	*ZnO length (μm)*
1	0.5	2	78	0.8
2	0.5	20	39	0.4
3	0.001	20	76	0.8
4	0.001	2	36	1.7
5	0.5	10	67	0.5
6	0.001	10	75	0.5
7	0.25	20	87	1
8	0.25	2	79	2.3
9	0.25	10	87	1.5
10	0.25	10	89	1.2
11	0.25	10	82	1.3

Table 4
Analysis of variance (ANOVA) for the regression model obtained from the central composite design (CCD) for the response yield.

	DF	*Sum of Squares*	*Mean Square*	*F Value*	*Prob > F*
BAC	*1*	*1.5*	*1.5*	*0.048*	*0.834*
j	*1*	*13.5*	*13.5*	*0.437*	*0.538*
*BAC*BAC*	*1*	*1081.10*	*1081.10*	*34.99*	*0.002*
j*j	*1*	*189.90*	*189.90*	*6.146*	*0.056*
*BAC*j*	*1*	*1560.25*	*1560.25*	*50.49*	*8.55E-4*
Error	*5*	*154.49*	*30.90*		
Lack of fit	*3*	*128.49*	*42.83*	*3.29*	*0.24*
Pure Error	*2*	*26*	*13*		
Total	*10*	*3358.18*			

2.3. Experimental design

A multivariate experimental design approach was employed to investigate the effects of stabilizer concentration and current density on the zinc electrolysis yield in a sodium carbonate solution, as well as on the size of the resulting ZnO structures. To ensure comparability among variables measured on different scales and to prevent variables with larger numerical ranges from disproportionately influencing the results, all factors were normalized through coding. This process involves defining the extremes of each variable's domain and assigning them coded values, typically −1 for the lowest and + 1 for the highest real values. The central value is then coded as 0. The experimental matrix, including both the real (uncoded) and coded variables, is presented in Table 1

In this study, the experiments were designed following a Central Composite Design (CCD) with two variables at three levels, in accordance with the principles of Response Surface Methodology (RSM). Generally, a CCD explores each factor at five levels, coded as -α, −1, 0, +1, and + α. When α is set to 1, the resulting configuration is known as a face-centered CCD, in which the number of levels is reduced to three for each factor. This specific configuration was adopted for our experimental setup, requiring 9 experimental points, thus 9 (single run) experiments with different combination of the independent variables [12]. The central point was tested in triplicate. A geometric representation of the experimental domain investigated is provided in the Supplementary Information (Fig. S1). The experiments were performed in random order to avoid systematic errors due to memory/time effects.

This quadratic model enables the analysis of both the individual effects of each factor and their potential interactions on the response. Thus, it allowed us to determine which factors have a statistically significant impact and whether the effect of one factor is influenced by changes in another (interaction effect). Then, the response surface equation was obtained through multivariate regression fitting as follows (Eq. 1):

$$Y = b_0 + b_1 x_1 + b_2 x_2 + b_3 x_1 x_2 + b_4 x_1^2 + b_5 x_2^2 + e \quad (1)$$

Where x_1 and x_2 are the independent variables (respectively BAC concentration and current density), b_0 the intercept, b_1 and b_2 the regression coefficients associated to x_1 and x_2, b_3 the regression coefficient related to the interaction among x_1 and x_2, b_4 and b_5 the regression coefficients associated to the quadratic terms of x_1 and x_2, and e holds the residuals of the model. The software CAT -Chemometric Agile Tool was used for computation of the model and for statistical evaluations [23]. The experimental conditions at the validation points for the lab-scale and scale-up syntheses of ZnO MRs are summarized in Table 2.

3. Results and discussion

The proposed hybrid method consists of two steps: electrochemical synthesis and thermal treatment, as described elsewhere [7–9]. During the electrolysis, the generation of OH^- leads to the constant increase of solution pH, starting from 8.5 (pH of 30 mM $NaHCO_3$ aqueous solution) up to cca. 11.5. In this step, a colloidal suspension of zinc hydroxycarbonates was prepared under alkaline conditions, conducive to the formation of stable zinc-based species. Following thermal treatment, pure ZnO was obtained. The experimental yield was estimated by measuring the mass difference of working electrodes (named respectively WE e CE) before and after the synthesis process (Eq. (2)).

$$m_{experimental} = \Delta m\,(WE) - \Delta m\,(CE) \quad (2)$$

The theoretical mass was calculated according to Faraday's law for a two-electron process, as expressed in Eq. (3), where I is the current intensity, Δt is the process duration, M_{Zn} is Zn atomic mass, Z is the number of electrons involved in the process, and F is the Faraday constant:

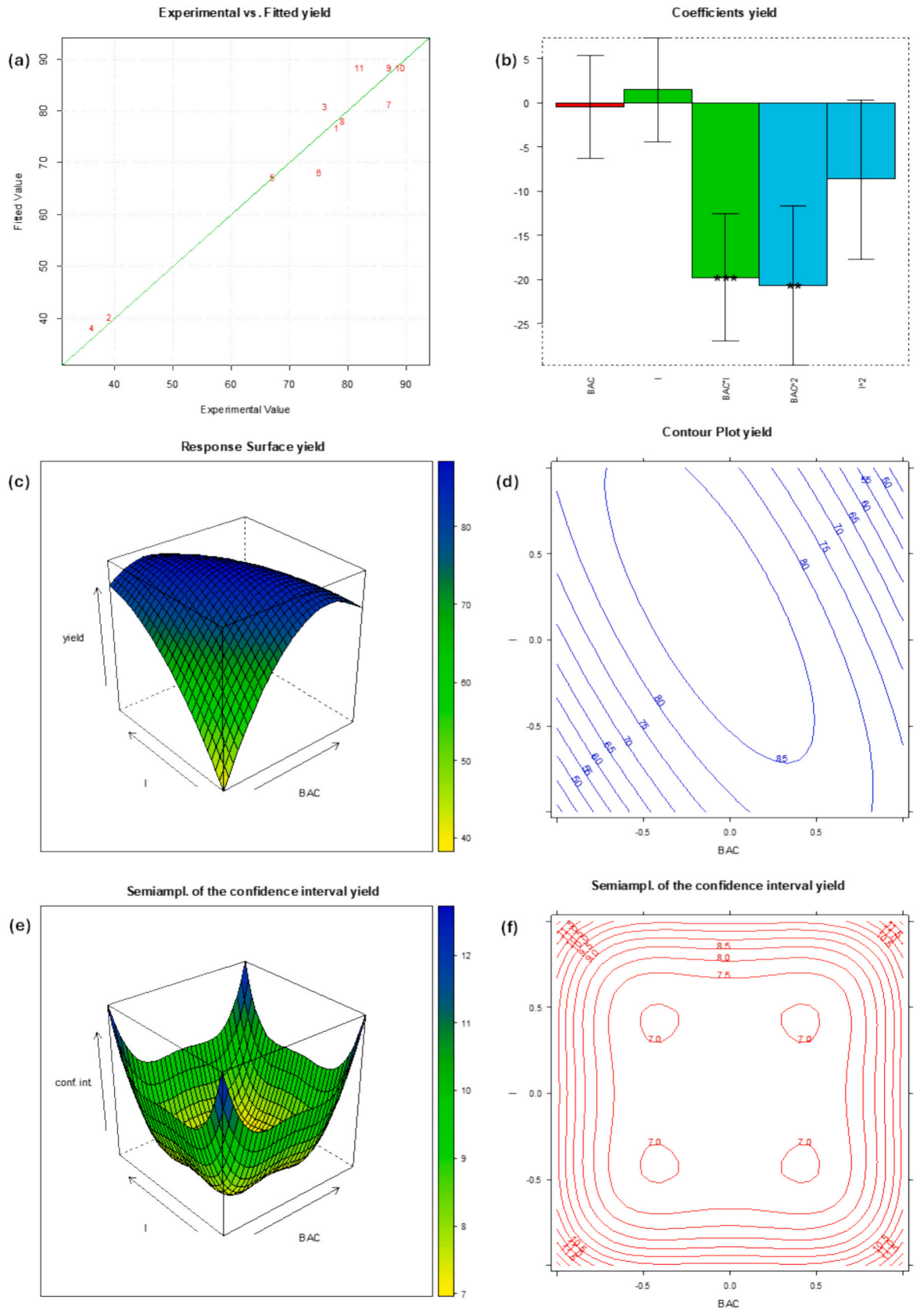

Fig. 1. Regression of the three-level Central Composite Design (CCD) model. (a) Predicted vs. actual values for synthesis yield. (b) Coefficients of the model equation. (c) Response surface of the yield as function of BAC concentration and current density and (d) relative contour plot. (e, f) Semi-amplitude of the confidence interval.

Table 5
Analysis of variance (ANOVA) for the regression model obtained from the central composite design (CCD) for the response yield.

	DF	Sum of Squares	Mean Square	F Value	Prob > F
BAC	1	0.282	0.282	4.195	0.0956
j	1	1.127	1.127	16.779	0.009
BAC*BAC	1	1.527	1.527	22.737	0.005
j*j	1	0.353	0.354	5.268	0.070
BAC*j	1	0.062	0.062	0.931	0.379
Error	5	0.336	0.067		
Lack of fit	3	0.290	0.096	4.129	0.201
Pure Error	2	0.047	0.023		
Total	10	3.410			

$$m_{theoretical} = \frac{M_{Zn}\ (g/mol) \bullet \Delta t\ (s) \bullet I\ (A)}{Z\ (eq/mol) \bullet F\ (C/eq)} \tag{3}$$

A face-centered CCD was employed to optimize the electrosynthesis yield of ZnO structures and to rationalize their size. Using a three-level CCD model, the effects of current density and BAC concentration on these system responses were systematically investigated. This approach resulted in nine points (Fig. S1), which were randomly conducted and are summarized in Table 3. The central point was tested in triplicate. The same table reports the yield obtained and the length of the elongated ZnO microstructures for each experiment.

By applying multiple regression analysis on the experimental data, a predictive quadratic polynomial model is developed and an equation to describe the correlation between the dependent variable (Y_i, in our case the yield and the ZnO length) and the independent variables (X_i, i.e. BAC concentration and current density) has been modeled.

For the yield, the resulting model equation is:

$$\text{Yield}\ (\%) = 88.3 - 0.5\ x_1 + 1.5\ x_2 - 19.7\ x_1x_2 - 20.6\ {x_1}^2 - 8.6\ {x_2}^2$$

The multiple linear regression (MLR) analysis yielded satisfactory results, with the model explaining 91 % of the variance in the dataset ($R^2 = 0.91$). The ANOVA results (Table 4) confirm the adequacy of the regression model, as the lack-of-fit test was not significant ($p = 0.24 > 0.05$ at a 95 % confidence level). The analysis of F-values further highlights that the quadratic term of [BAC] and the interaction between [BAC] and current density (j) exhibit the most significant effects on the response.

Fig. 1a displays the correlation between experimental and predicted values, confirming the robustness of the model fit. Fig. 1b highlights the statistically significant regression coefficients, notably the interaction term between [BAC] and current density (j), as well as the quadratic term of [BAC]. The interaction term was statistically significant at the 99.9 % confidence level ($p = 0.001$) and exhibited a negative coefficient, indicating that the electrosynthetic yield decreases as the product of [BAC] and j increases. Similarly, the quadratic term of [BAC] was significant at the 99 % confidence level ($p = 0.01$), revealing a non-linear relationship. The negative coefficient suggests that while moderate [BAC] concentrations enhance the yield, excessive concentrations have a detrimental effect. Although a similar quadratic effect might be anticipated for current density, its corresponding coefficient was not statistically significant. This lack of significance, accompanied by wide confidence intervals, is likely attributable to the limited degrees of freedom in the model. The response surface illustrated in Fig. 1c demonstrates an almost linear increase in electrosynthetic yield with increasing current density. In contrast, the yield increases with [BAC] concentration only up to an optimal value, beyond which further increases result in a decline. This trend defines an optimal region in the experimental design space, where the synthetic yield reaches approximately 90 %. As shown more clearly by the isoresponse curves in Fig. 1d, this optimal region corresponds to [BAC] concentrations ranging from 0.15 M (coded value: −0.4) to 0.3 M (coded value: 0.25).

Following the rationalization and optimization of the electrosynthesis yield of ZnO microrods (MRs), the investigation was subsequently directed toward their length. While this type of measurement is inherently associated with greater uncertainty due to its basis in statistical size analysis of TEM micrographs, we nevertheless attempt to model the system's behavior as a function of current density and BAC concentration. In this case, it is not appropriate to define an optimum value, as this depends on the specific requirements of the application, particularly whether shorter or longer rods are preferred. Therefore, it is more appropriate to state that this rationalization study serves as a useful tool to directly tailor the ZnO particle size according to the intended application. For the length of ZnO MRs, the resulting model equation is:

$$\text{ZnO length}\ (\mu m) = 1.28 - 0.217\ x_1 - 0.43\ x_2 + 0.125\ x_1x_2 - 0.76\ {x_1}^2 + 0.39\ {x_2}^2$$

The MLR analysis resulted in an explained variance of 78 %, a satisfactory result considering the intrinsic higher uncertainty of the response values on which the model was based. The ANOVA results (Table 5) demonstrate that the regression model is statistically adequate, as the lack-of-fit test was not significant ($p = 0.20 > 0.05$ at the 95 % confidence level). Moreover, the F-value analysis indicates that the current density (j) and the quadratic term of [BAC] have the most significant influence on the response.

As shown in Fig. 2a, the model fits the experimental trend with good agreement. The factors found to be significant in influencing the length of ZnO are the current density (j) at the 95 % confidence level ($p = 0.05$), and the quadratic term of the BAC concentration at the 99 % confidence level ($p = 0.01$) (Fig. 2b). Among the factors considered, the latter has the most substantial impact on ZnO length, presenting the highest coefficient value. The second-highest coefficient corresponds to the current density and is negative, indicating that ZnO length decreases with increasing current density. As shown more clearly in the response surface depicted in Fig. 2c, the length of the ZnO microrods decreases with increasing current density. This is in agreement with the effects of more chaotic processes occurring at higher current densities, conflicting with the template effects exerted by the quaternary ammonium capping agent. The effect of BAC concentration is non-linear: the particle length increases up to a maximum around a coded value of −0.20 (corresponding to 0.2 M), after which it decreases. Lower current densities combined with a BAC concentration of ~0.2 M resulted in the longest ZnO structures (Fig. 2d). It is noteworthy that, in this case, it is difficult to identify a robust region on the response surface, indicating that the ZnO length is highly sensitive to small changes in the experimental conditions and is therefore strongly condition-dependent.

3.1. Validation at laboratory scale

The models that provided statistically satisfactory results were further validated through three independent experiments, conducted outside the dataset used for the model development. These experiments were selected within the central robust region of the design space; however, the exact center point (coordinates [0,0]) could not be used, as it had already been included in the CCD. Therefore, the point corresponding to [BAC] = −0.5 and j = 0.5 was selected (depicted in Fig. S2 and S3), which corresponds to a BAC concentration of 0.1 M and a current density of 15.5 mA/cm^2. Table 6 reports the experimental yield and ZnO length for the three replicates, along with the corresponding averages and confidence intervals. The observed variability in the electrochemical yield is likely due to experimental conditions (e.g. recovery of the material, cleanliness of the zinc sheets). To assess the agreement between experimental and predicted values, a *t*-test was performed (see Supporting Information for details), comparing the experimental results with the model prediction and its confidence interval (which are shown in Fig. 1e,f and Fig. 2e,f for yield and ZnO length, respectively) at the selected point. The resulting *t*-value indicates

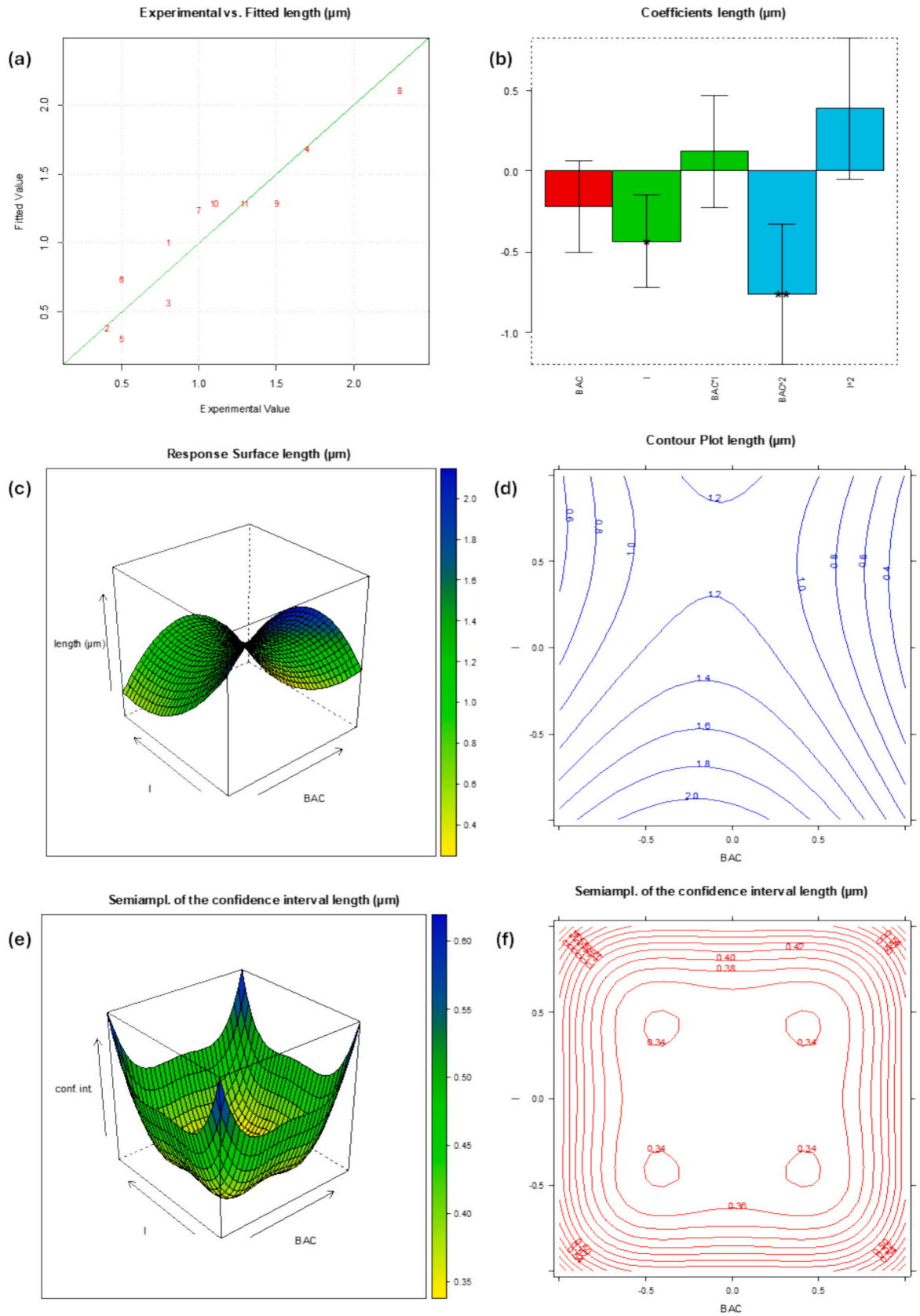

Fig. 2. Regression of the three-level Central Composite Design (CCD) model. (a) Predicted vs. actual values for ZnO length. (b) Coefficients of the model equation. (c) Response surface of the ZnO length as function of BAC concentration and current density and (d) relative contour plot. (e, f) Semi-amplitude of the confidence interval.

Table 6
Validation of the models at the point −0.5,0.5 of the domain, corresponding to BAC concentration of 0.1 M and current density of 15.5 mA/cm^2.

Reps.	Experimental yield (%)	Average and conf. Int. (%)	Predicted value and conf. Int. (%)	Experimental ZnO length (μm)	Average and conf. Int. (%)	Predicted value and conf. Int. (%)
1	90			0.9		
2	85	86 ± 9	89 ± 7	1.2	1.1 ± 0.4	1.1 ± 0.3
3	83			1.1		

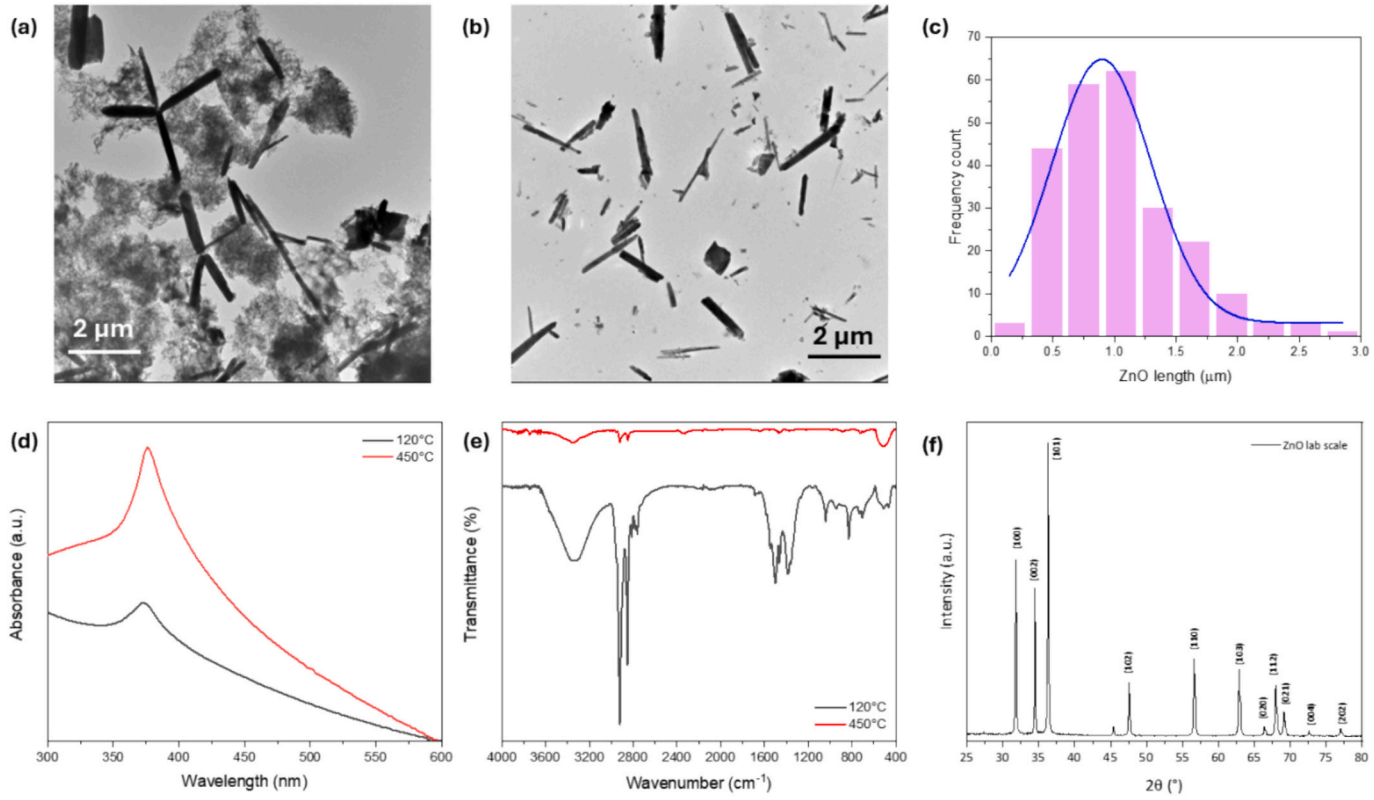

Fig. 3. TEM micrographs (scale bar 2 μm) of ZnO microrods synthesized with BAC concentration of 0.1 M and a current density of 15.5 mA/cm^2, after drying at 120 °C (a) and calcination at 450 °C (b); size analysis of the ZnO length by ImageJ software (c). UV–Vis spectra of ZnO MR dispersions (d); and FTIR spectra of ZnO powders (e). XRPD of the calcinated ZnO powder (f).

no statistically significant difference between predicted and experimental results at the 95 % confidence level and with 2 degrees of freedom. Therefore, it can be concluded that the model is validated.

ZnO MRs synthesized at validation point were morphologically and spectroscopically characterized after drying and calcination thermal treatments. In fact, as reported elsewhere [8], the latter guaranteed the complete conversion of the as-prepared colloidal materials into stoichiometric ZnO species without large morphological modification. TEM images reported in Fig. 3 a,b showed rod-like structures, with an average length of 1.1 ± 0.4 μm for the sample dried at 120 °C (Fig. 3 c). UV–Vis spectra of the samples exhibited typical absorption peak of microstructured ZnO around 375 nm [24]. The calcination process induced an increase in peak intensity, due to conversion into stoichiometric ZnO, resulting into increased absorption. IR data indicate that ZnO is already present in the samples dried at 120 °C, as evidenced by the characteristic IR band in the 440–500 cm^{-1} region, which is attributed to Zn—O stretching vibrations [25]. The spectral region between 1300 and 1600 cm^{-1}, typically associated with hydrozincite-like species ($Zn_x(CO_3)_y(OH)_z$) [26], shows a noticeable decrease in intensity after calcination. Moreover, increasing the treatment temperature leads to the disappearance of C—H stretching signals at 3000–2800 cm^{-1} [27]. In contrast, the bands corresponding to styrene/carbonyl functionalities (1700–1600 cm^{-1}) slightly increase upon calcination. This behavior may be attributed to the thermal degradation of BAC, resulting in the formation of carbonaceous residues. The diffraction pattern (Fig. 3f) revealed reflections characteristic of the hexagonal wurtzite structure of ZnO. Phase identification was performed using the QualX software [28] by correlating the experimental XRPD data with the reference database (# 00–900-4178) and calculating the associated d-spacing values, which are listed in Table S1 of the Supporting Information.

3.2. *Validation at scale up*

The electrosynthesis method presented in this work is readily scalable for industrial applications. By increasing the electrode area, the volume of the electrolyte, and the duration of the synthesis, it is possible to produce ZnO particles in quantities easily exceeding the gram-scale. Zinc is a cost-effective material, and the electrolyte consists primarily of a bicarbonate solution, making the scaling-up process economically and practically viable. Given that the theoretical principles underlying the electrochemical synthesis are consistent across both laboratory and scaled-up conditions, we sought to evaluate whether the model developed from lab-scale experiments could be extrapolated to larger-scale syntheses. To this end, we tested the predictive capability of the regression models for both yield and particle size by applying them to a new experimental condition within the scaled-up configuration, as

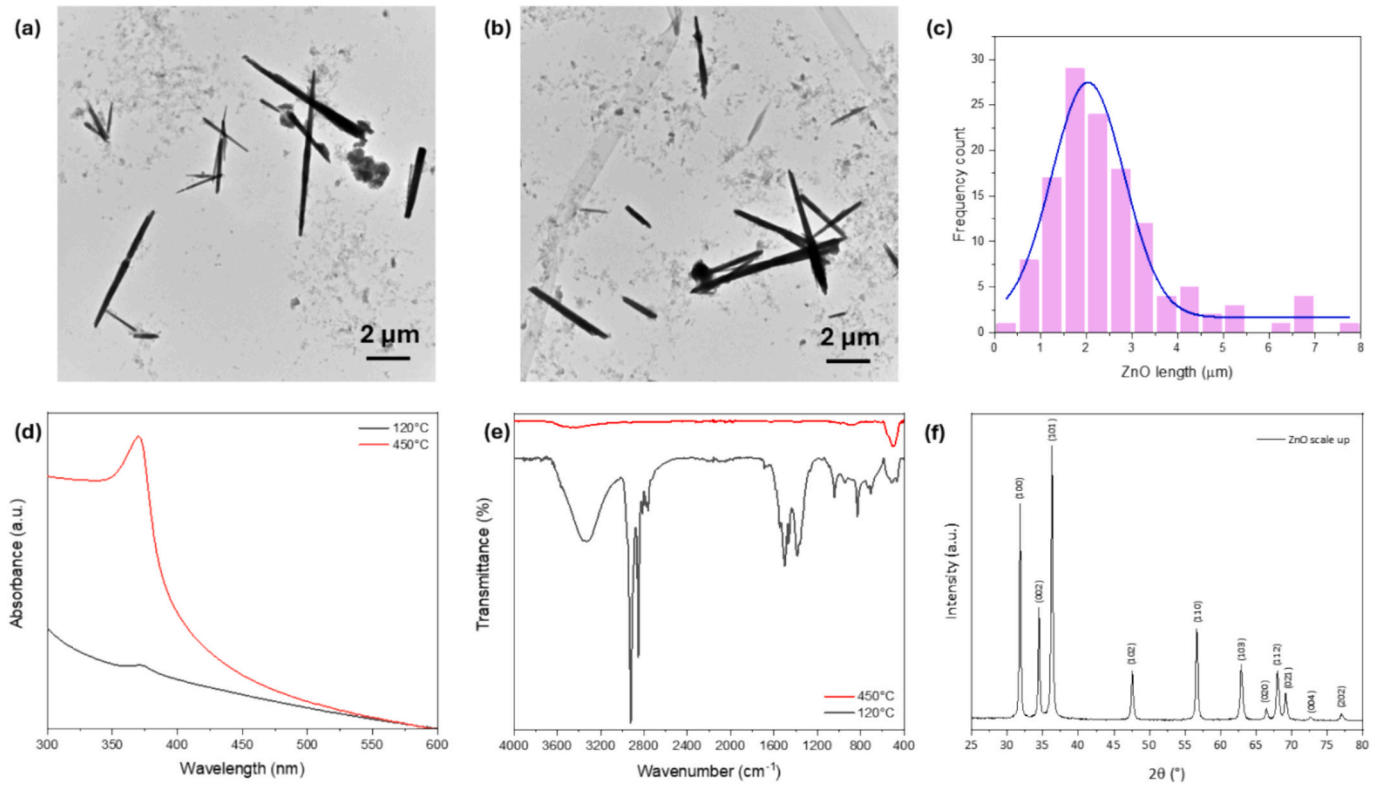

Fig. 4. TEM micrographs (scale bar 2 µm) of ZnO microrods synthesized with a scaled setup, with BAC concentration of 0.01 M and a current density of 10 mA/cm^2, after drying at 120 °C (a) and calcination at 450 °C (b); size analysis of the ZnO length by ImageJ software (c). UV–Vis spectra of ZnO microstructure dispersions (d); and FTIR spectra of ZnO powders (e). XRPD of the calcinated ZnO powder (f).

detailed in the Experimental Section. The scale-up electrosynthesis was conducted over 3 h, using a BAC concentration of 0.01 M (coded value: −0.96) and a current density of 10 mA/cm^2 (coded value: −0.1). According to Faraday's law, the theoretical mass of ZnO expected from the electrolysis is 0.9 g. Experimentally, a mass of 0.69 g was obtained, corresponding to a synthetic yield of 75 %. This value falls within the confidence interval of the predicted yield, which was 69 ± 13 %. These findings thereby confirm that the lab-scale rationalization remains valid under scale-up conditions.

However, slight deviations were observed between the predicted and experimental particle sizes. According to Fig. 4c, the size analysis of the ZnO structures obtained from TEM images (Fig. 4a,b) revealed an average particle length of 2.0 ± 0.9 µm, which seems not align completely with the predicted size of 0.9 ± 0.5 µm under the same experimental conditions. However, it should be noted that the length model is subject to greater variability due to the intrinsic uncertainty in the response values, as previously discussed. Specifically, the error arises from the statistical analysis of particle sizes measured from TEM micrographs, where the size distribution is obtained through fitting, a procedure inherently associated with larger uncertainty. Furthermore, physical transport phenomena (e.g., convection or electrode dynamics) may have a more significant role at larger scales. Indeed, it was reported that reduced convection and limited ion transport can favor the growth of existing ZnO crystallites, leading to larger particle sizes [29]. The UV–Vis and IR spectroscopic characterizations (Fig. 4 d,e) present the typical features of microstructured ZnO particles, already detailed above. Similarly to the previous sample, the diffraction peaks (Fig. 4f) revealed signals characteristic of the hexagonal wurtzite structure of ZnO.

4. Conclusions

In this study, we presented for the first time the application of a two-factor, three-level Central Composite Design (CCD) combined with Response Surface Methodology (RSM) to optimize both the electrosynthetic yield and morphological characteristics (length) of ZnO microrods. While the influence of experimental parameters on ZnO electrochemical synthesis has been explored by an OVAT approach in previous research, the present work introduces a novel chemometric framework that enables a quantitative, multivariate analysis of the system, thus moving beyond traditional empirical approaches. By investigating two critical parameters, i. e. the concentration of benzalkonium chloride (BAC) used as the particle stabilizing agent and the applied current density, we successfully mapped the response surfaces and identified optimal conditions for maximizing synthetic yield and controlling the structure dimensions by means of just 11 experiments (9 points, with three replicates in the central point). The yield was found to increase linearly with current density and to reach a maximum within a defined BAC concentration range (0.15–0.3 M), achieving values close to 90 %. Despite the intrinsic uncertainty associated with the ZnO rod length values, it was possible to successfully build a model that explained the response trend. The ZnO rod length decreased with increasing current density, while BAC concentration exhibited a non-linear effect, with a maximum value around 0.2 M. The robustness and predictive power of the developed models were validated through targeted experiments both at the laboratory scale and under scaled-up conditions. For the lab-scale validation, three independent replicates confirmed good agreement between experimental and predicted outcomes for both yield and size, with no statistically significant differences

(95 % confidence level, 2 degrees of freedom). Under scale-up conditions, the model accurately predicted the process yield and provides a good trend for the ZnO length.

Overall, this work demonstrates a powerful and transferable strategy for the rational optimization of electrochemical synthesis processes, supporting both scientific understanding and technological scalability. The integration of DoE and RSM into materials synthesis offers a sustainable, efficient, and industrially relevant methodology that can be extended to other materials and electrochemical systems.

CRediT authorship contribution statement

Margherita Izzi: Writing – review & editing, Writing – original draft, Validation, Resources, Methodology, Investigation, Formal analysis. **Alessandro Faranda:** Investigation. **Rosaria Anna Picca:** Writing – review & editing, Supervision. **Gennaro Ventruti:** Investigation, Writing – review & editing. **Barbara Giussani:** Writing – review & editing, Supervision, Methodology, Conceptualization. **Nicola Cioffi:** Writing – review & editing, Supervision, Resources, Conceptualization.

Declaration of competing interest

The authors declare that they have no known competing financial interests or personal relationships that could have appeared to influence the work reported in this paper.

Acknowledgements

M.I. acknowledges the financial support from the ERC SEEDS UNIBA programme, project H93C23000660001, “REAL - More for less: REthinking AntimicrobiaL materials”.

Appendix A. Supplementary data

Supplementary data to this article can be found online at https://doi.org/10.1016/j.inoche.2025.115818.

Data availability

Data will be made available on request.

References

[1] A.U. Hasanah, P.L. Gareso, N. Rauf, D. Tahir, Photocatalytic performance of zinc oxide and metal-doped zinc oxide for various organic pollutants, Chem. Bio Eng. Rev. 10 (2023) 698–710, https://doi.org/10.1002/cben.202300004.
[2] R.T. Hussain, M.S. Hossain, J.H. Shariffuddin, Green synthesis and photocatalytic insights: a review of zinc oxide nanoparticles in wastewater treatment, Mater Today Sustain 26 (2024) 100764, https://doi.org/10.1016/j.mtsust.2024.100764.
[3] B.G. Prajapati, D. Sharma, G.M. Elossaily, N. Sharma, A. Bilandi, D.U. Kapoor, Unlocking potential of zinc oxide nanoparticles in enhancing topical drug delivery, Nano-Struct. Nano-Obj. 39 (2024) 101302, https://doi.org/10.1016/j.nanoso.2024.101302.
[4] M. Izzi, M.C. Sportelli, L. Torsi, R.A. Picca, N. Cioffi, Synthesis and antimicrobial applications of ZnO nanostructures: a review, ACS Appl. Nano Mater. 6 (2023) 10881–10902, https://doi.org/10.1021/acsanm.3c01432.
[5] K. Bachhav, A.S. Garde, Versatile synthesis of zinc oxide nanoparticles via chemical route: a review, Mater Today Proc 103 (2024) 228–236, https://doi.org/10.1016/j.matpr.2023.08.269.
[6] M. Parashar, V.K. Shukla, R. Singh, Metal oxides nanoparticles via sol–gel method: a review on synthesis, characterization and applications, J. Mater. Sci. Mater. Electron. 31 (2020) 3729–3749, https://doi.org/10.1007/s10854-020-02994-8.
[7] R.A. Picca, M.C. Sportelli, D. Hötger, K. Manoli, C. Kranz, B. Mizaikoff, L. Torsi, N. Cioffi, Electrosynthesis and characterization of ZnO nanoparticles as inorganic component in organic thin-film transistor active layers, Electrochim. Acta 178 (2015) 45–54, https://doi.org/10.1016/j.electacta.2015.07.122.
[8] M.C. Sportelli, R.A. Picca, M. Izzi, G. Palazzo, R. Gristina, M. Innocenti, L. Torsi, N. Cioffi, ZnO nanostructures with antibacterial properties prepared by a green electrochemical-thermal approach, Nanomaterials 10 (2020) 473, https://doi.org/10.3390/nano10030473.
[9] R.A. Picca, M.C. Sportelli, R. Lopetuso, N. Cioffi, Electrosynthesis of ZnO nanomaterials in aqueous medium with CTAB cationic stabilizer, J. Sol-Gel Sci. Technol. 81 (2017) 338–345, https://doi.org/10.1007/s10971-016-4268-9.
[10] E.M. Williamson, Z. Sun, L. Mora-Tamez, R.L. Brutchey, Design of experiments for nanocrystal syntheses: a how-to guide for proper implementation, Chem. Mater. 34 (2022) 9823–9835, https://doi.org/10.1021/acs.chemmater.2c02924.
[11] B. Benedetti, Caponigro, F. Vicky, Ardini, Experimental design step by step: a practical guide for beginners, Crit. Rev. Anal. Chem. 52 (2022) 1015–1028, https://doi.org/10.1080/10408347.2020.1848517.
[12] R. Leardi, Experimental design in chemistry: a tutorial, Anal. Chim. Acta 652 (2009) 161–172, https://doi.org/10.1016/j.aca.2009.06.015.
[13] M.A. Bezerra, R.E. Santelli, E.P. Oliveira, L.S. Villar, L.A. Escaleira, Response surface methodology (RSM) as a tool for optimization in analytical chemistry, Talanta 76 (2008) 965–977, https://doi.org/10.1016/j.talanta.2008.05.019.
[14] H.-D. So, S.-H. Jon, W.-C. Yang, Process optimization for electrochemical synthesis of ZnO nanoparticles with respect to productivity and consumption using TOPSIS and Taguchi methods, Sci. Rep. 15 (2025) 16619, https://doi.org/10.1038/s41598-025-01833-2.
[15] V. Anand, V.C. Srivastava, Zinc oxide nanoparticles synthesis by electrochemical method: optimization of parameters for maximization of productivity and characterization, J. Alloys Compd. 636 (2015) 288–292, https://doi.org/10.1016/j.jallcom.2015.02.189.
[16] M. Ramezani, S.M. Pourmortazavi, M. Sadeghpur, A. Yazdani, I. Kohsari, Silver tungstate nanostructures: electrochemical synthesis and its statistical optimization, J. Mater. Sci. Mater. Electron. 26 (2015) 3861–3867, https://doi.org/10.1007/s10854-015-2912-8.
[17] S.M. Pourmortazavi, M. Rahimi-Nasrabadi, Y. Fazli, M. Mohammad-Zadeh, Taguchi method assisted optimization of electrochemical synthesis and structural characterization of copper tungstate nanoparticles, Int. J. Refract. Met. Hard Mater. 51 (2015) 29–34, https://doi.org/10.1016/j.ijrmhm.2015.02.013.
[18] Y. Fazli, S. Mahdi Pourmortazavi, I. Kohsari, M. Sadeghpur, Electrochemical synthesis and structure characterization of nickel sulfide nanoparticles, Mater. Sci. Semicond. Process. 27 (2014) 362–367, https://doi.org/10.1016/j.mssp.2014.07.013.
[19] R.G. Brereton, Experimental design, in: Chemometrics: Data Analysis for the Laboratory and Chemical Plant, Chapter 2, John Wiley & Sons Ltd, 2003, pp. 15–117, https://doi.org/10.1002/0470863242.ch2.
[20] L.G. de Oliveira, A.P. de Paiva, P.P. Balestrassi, J.R. Ferreira, S.C. da Costa, P.H. da Silva Campos, Response surface methodology for advanced manufacturing technology optimization: theoretical fundamentals, practical guidelines, and survey literature review, Int. J. Adv. Manuf. Technol. 104 (2019) 1785–1837, https://doi.org/10.1007/s00170-019-03809-9.
[21] E.R.V. Almeida, A.S. Melo, A.S. Lima, V.A. Lemos, G.S. Oliveira, C.F. Cletche, A. S. Souza, M.A. Bezerra, A review of the use of central composite design in the optimization of procedures aiming at food chemical analysis, Food Chem. 480 (2025) 143849, https://doi.org/10.1016/j.foodchem.2025.143849.
[22] O. Gerard, M.N. Mustafa, S. Ramesh, K. Ramesh, A. Numan, Y.S. Tan, S.K. Tiong, S. Ramesh, M. Khalid, Central composite design optimization of cobalt-copper phosphate binderless battery-grade electrode via electrodeposition technique, Electrochim. Acta 532 (2025) 146471, https://doi.org/10.1016/j.electacta.2025.146471.
[23] R. Leardi, C. Melzi, G. Polotti, CAT (Chemometric Agile Tool). http://gruppochemiometria.it/index.php/software, 2024.
[24] R. Al-Gaashani, S. Radiman, A.R. Daud, N. Tabet, Y. Al-Douri, XPS and optical studies of different morphologies of ZnO nanostructures prepared by microwave methods, Ceram. Int. 39 (2013) 2283–2292, https://doi.org/10.1016/j.ceramint.2012.08.075.
[25] S. Musić, S. Popović, M. Maljković, Đ. Dragčević, Influence of synthesis procedure on the formation and properties of zinc oxide, J. Alloys Compd. 347 (2002) 324–332, https://doi.org/10.1016/S0925-8388(02)00792-2.
[26] M.C. Hales, R.L. Frost, Synthesis and vibrational spectroscopic characterisation of synthetic hydrozincite and smithsonite, Polyhedron 26 (2007) 4955–4962, https://doi.org/10.1016/j.poly.2007.07.002.
[27] N.O. of D. and Informatics, NIST Chemistry WebBook, (n.d.). Doi: 10.18434/T4D303.
[28] A. Altomare, N. Corriero, C. Cuocci, A. Falcicchio, A. Moliterni, R. Rizzi, QUALX2.0: a qualitative phase analysis software using the freely available database POW_COD, J. Appl. Crystallogr. 48 (2015) 598–603, https://doi.org/10.1107/S1600576715002319.
[29] F. Bittner, T. Oekermann, M. Wark, Scale-up of the electrodeposition of ZnO/eosin Y hybrid thin films for the fabrication of flexible dye-sensitized solar cell modules, Materials 11 (2018) 232, https://doi.org/10.3390/ma11020232.

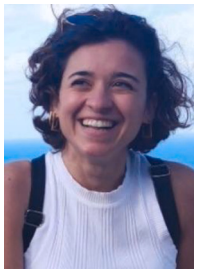

Margherita Izzi received her PhD in Chemical and Molecular Sciences from the University of Bari Aldo Moro in 2022. Her interdisciplinary research focuses on the design, synthesis, and characterization of functional nanomaterials with antimicrobial and antiviral properties. She has expertise in developing nanocomposites for food packaging and cultural heritage applications, applying chemometric tools for material rationalization and optimization, and, more recently, investigating antimicrobial mechanisms at the early stages of interaction with microorganisms.

Alessandro Faranda obtained his bachelor's degree in Chemistry summa cum laude from the University of Bari (Italy) in 2024. He is currently pursuing a master's degree in Industrial Chemistry at the same university.

Rosaria Anna Picca is Associate Professor of Analytical Chemistry at the Chemistry Department of the University of Bari Aldo Moro since Dec 2021. She has almost 20 years of experience in the preparation and characterization of nanocomposites of applications in different fields, from antimicrobial coatings to sensors. She has focused on the investigation of green methods (including electrochemical ones) for nanomaterial synthesis and in the development of biopolymer-based films. She is co-author of more than 100 publications and 5 book chapters.

Gennaro Ventruti is an Associate Professor of SSD GEO/06 at the Department of Earth and Geoenvironmental Sciences, University of Bari. His primary research focuses on the characterization of materials for sustainable and environmental applications. He specializes in the study of minerals and synthetic materials using spectroscopic and diffraction techniques, including studies conducted under non-ambient conditions.

Barbara Giussani graduated in Chemistry from the University of Insubria (Como, Italy) in 2001 and obtained her Ph.D. in Analytical Chemistry from the same university in 2004. She is currently an Associate Professor at the Department of Science and High Technology, where she teaches Analytical Chemistry and Chemometrics. Her research focuses on chemometrics, process control strategies, and the development of smart analytical approaches for real-world applications, from sampling to data interpretation. She mainly employs infrared and near-infrared spectroscopy, particularly with portable sensors, and her current interests include multivariate error and model uncertainty estimation.

Nicola Cioffi, PhD, is full professor of Analytical Chemistry at the Chemistry Department of the University of Bari, Italy, since 2018. Past-coordinator of the Italian Analytical Spectroscopy Board (Italian Chemical Society, SCI), Treasurer of the SCI Analytical Chemistry Division, he is member of the Italian CSGI consortium (Research Center for Colloids and surface science), and, since 2018, he coordinates the Bari unit. Since 2017, he has also been co-chair of the CHESS international School on Surface Analysis. Since 2019, he is one of the editors of Analytica Chimica Acta. His research interests are in the fields of (i) Surface chemistry and Spectroscopy (ii) Nanomaterials for the life sciences, including nanoantimicrobials, (iii) Sensors.